This is a preprint, the final version is subject to change, of the American Mineralogist (MSA)
Cite as Authors (Year) Title. American Mineralogist, in press.
(DOI will not work until issue is live.) DOI: http://dx.doi.org/10.2138/am.2014.4442

(Revision 2)

Electrical conductivity of synthetic mullite single crystals

Mohammed Malki[1,2*], Jürgen Schreuer[3] and Hartmut Schneider[4,5]

[1] CEMHTI, Conditions Extrêmes et Matériaux: Haute Température et Irradiation, CNRS UPR 3079, 1D avenue de la Recherche Scientifique, 45071 Orléans cedex 2, France.

[2] Ecole Polytechnique de l'Université d'Orléans, 45072 Orléans, France.

[3] Institut für Geologie, Mineralogie und Geophysik, Ruhr-Universität Bochum, Universitätsstrasse 150, 44801 Bochum, Germany.

[4] Institut für Kristallographie, Universität zu Köln, Greinstrasse 6, 50939 Köln, Germany

[5] Fachbereich Geowissenschaften, Universität Bremen, Klagenfurter Strasse, 28334 Bremen, Germany

*Corresponding author:
E-mail: mohammed.malki@univ-orleans.fr
Tel.: +33 2 38 25 76 83
Fax: +33 2 38 63 81 03

Always consult and cite the final, published document. See http://www.minsocam.org or GeoscienceWorld

This is a preprint, the final version is subject to change, of the American Mineralogist (MSA)
Cite as Authors (Year) Title. American Mineralogist, in press.
(DOI will not work until issue is live.) DOI: http://dx.doi.org/10.2138/am.2014.4442

ABSTRACT

The electrical conductivity of 2/1-mullite (approximate composition $2Al_2O_3 \cdot SiO_2$) was measured using plane parallel, polished plates cut perpendicular to [100], [010] and [001] from a large single crystal grown by the Czochralski method. Impedance spectra were recorded in the 1 Hz to 1 MHz frequency range at temperatures from 550 °C to 1400 °C in air. The conductivity versus temperature curves display changes of their slope between 850 °C and 950 °C depending on the crystallographical direction. The low temperature region ($T <$ 850 °C) of conductivity is characterized by low electrical conductivities ($\sigma_{av.} \approx 5.4 \cdot 10^{-9}$ $\Omega^{-1}cm^{-1}$, average conductivity at 550°C) with $\sigma_{[010]} > \sigma_{[100]} > \sigma_{[001]}$ and low activation energies (≈ 0.66 eV, average value). In the high temperature region ($T >$ 950 °C) the electrical conductivity is significantly higher ($\sigma_{av} \approx 1.1 \cdot 10^{-5}$ $\Omega^{-1}cm^{-1}$, average conductivity at 1400 °C) with $\sigma_{[001]} > \sigma_{[100]} \approx \sigma_{[010]}$, and with higher activation energies (≈ 1.6 eV). While the conductivity in the low temperature region essentially is electronic, ion conductivity dominates the conductivity in the high temperature region. We believe that the ionic conductivity is essentially due to hopping of oxygen atoms from structural sites linking the tetrahedral double chains in mullite towards adjacent oxygen vacancies especially in **c**-axis direction. These oxygen hoppings are associated with complex structural re-arrangements, which control and slow down the velocity of the processes. Thus the electrical conductivity of mullite at high temperature is much lower than e.g. that of Y-doped zirconia, but is significantly higher than that of α-alumina.

Keywords: mullite, single crystals, electrical conductivity, high temperature

Always consult and cite the final, published document. See http://www.minsocam.org or GeoscienceWorld

INTRODUCTION

In spite of the fact that mullite occurs only very seldomly in natural rocks it is certainly one of the most widely studied materials in oxide ceramics. This is due to its outstanding properties, especially at high temperatures. Among these properties are the high thermal and chemical stability and the excellent thermo-shock and creep behavior which make mullite a promising candidate for many high temperature applications (see e.g. Schneider and Komarneni, 2005, and the references therein).

The crystal structure of mullite can best be described by means of the structurally closely related but more simple sillimanite. The key features of the crystal structure of sillimanite (Figure 1) are edge-sharing octahedral AlO_6 chains running parallel to the **c**-axis (Fischer and Schneider, 2005). The octahedral chains are linked by double chains of corner-sharing MO_4 tetrahedra (also parallel **c**), with an ordered distribution of the tetrahedral cations Al^{3+} and Si^{4+}. Perpendicular to the **c**-axis the situation is different, with a sequence of AlO_6 octahedra and AlO_4 and SiO_4 tetrahedra occurring parallel to the **a**- and **b**-axis (Figure 1). The average structure of mullite can be derived from the one of sillimanite by the coupled substitution Si^{4+}_{tet} by Al^{3+}_{tet} (tet = tetrahedral) and simultaneous Al^{3+} and Si^{4+} disordering over the tetrahedral sites. The excess negative charge in mullite produced by the substitution of Si^{4+} by Al^{3+} is compensated by the formation of oxygen vacancies (see e.g. Fischer and Schneider, 2005). It involves removal of oxygens bridging two adjacent tetrahedra in the sillimanite structure (O(C) oxygen atoms), with the number of vacancies corresponding to the x-value of the general formula of the mullite-type alumino silicates $Al_{4+2x}Si_{2-2x}O_{10-x}$. The formation of vacancies causes associated tetrahedral sites TS to be displaced to positions designated as TS*, so that the formerly bridging O(C) oxygen atoms become threefold coordinated and form T_3O groups (the so-called tetrahedral triclusters, TS*, according to literature the TS position is favorably occupied by Al, see Figure 1).

Always consult and cite the final, published document. See http://www.minsocam.org or GeoscienceWorld

A few preliminary studies exist on the electrical conductivity of mullite at high temperatures. Rommerskirchen et al. (1994), on the basis of electromagnetic fields (EMF) measurements on mullite ceramics provided data for an extremely high ionic conductivity of mullite being even superior to that of CaO-stabilized ZrO_2 solid electrolytes at temperatures between 1400°C and 1600°C. Chaudhuri et al. (1999) carried out DC (direct current) measurements to determine the electrical resistivity of undoped and transition metal-doped mullite ceramics at 1400°C. Chaudhuri and coworkers found a much lower electrical conductivity lying in between those of α-alumina and CaO-doped zirconia. Results of Faradaic current studies published by Mata-Osoro et al. (2012) at voltages up to 1000 V on mullite single crystals, ceramics and cermets showed small but measurable currents even at room temperature.

The determination of the nature of charge carriers in highly resistive materials is a challenge in general. For mullite, it has been suggested that below about 1000 °C, n-type electronic conduction might be expected to dominate (Buchanan, 2004). Using *ab initio* calculations, Aryal et al. (2012) showed that the 2/1-mullite single crystal is a large band gap insulator with a direct gap at the Brillouin zone center of about 4 eV. Analyzing the temperature dependence of the mullite resistivity up to 1400 °C, Chaudhuri et al. (1999) stated that mullite behaves like a non-metallic electrical conductor because its conductivity rises faster at low temperature but slows down at high temperature. Finally, Rommerskirchen et al. (1994) claimed that the mullite conductivity is predominantly ionic in the temperature range 1400 °C - 1600 °C.

As far as we know this is the first study performed on the electrical conductivity of mullite single crystals at high temperatures (up to 1400 °C) and also the first time that electrical conductivity of mullite is measured using impedance spectroscopy. The analysis of frequency dependence using impedance spectroscopy provides information about the dc-conductivity and can also give information on the nature of charge carriers in the samples.

Always consult and cite the final, published document. See http://www.minsocam.org or GeoscienceWorld

EXPERIMENTAL

Sample preparation

Mullite single crystals of about 2/1-composition ($2Al_2O_3 \cdot SiO_2$) were grown by P. Reiche (Institute of Crystal Growth, IKZ Berlin, Germany). The starting materials were highly pure Al_2O_3 (77.3 wt.%) and SiO_2 (22.7 wt.%) powders which were homogeneously mixed and subsequently melted. Colorless single crystals of high optical quality with dimensions up to 80 mm in length and 20 mm in diameter were obtained employing the Czochralski method (for details see Guse and Mateika, 1974). According to infrared spectroscopic analysis the mullite single crystal is unhydrous (Rüscher et al., 2002). Plane parallel single crystal discs being about 1 mm thick and with about 1 cm^2 surface were cut perpendicular to [100], [010] and [001] from one single crystal, and were subsequently polished.

Electrical conductivity

Impedance spectra were recorded on the samples using a Solartorn SI 1260 spectrometer in the frequency range 1 Hz to 1 MHz and in the temperature range 550 °C - 1400 °C under air. The electrodes were platinum foils held in contact with the surface sample by a weak mechanical pressure controlled by a spring system and transmitted to the sample using an alumina rod. The sample was placed in the central zone of a vertical tubular furnace where the temperature is uniform. The temperature of the sample was measured using a Pt/Pt-10%Rh thermocouple located near the sample with an uncertainty of ± 20 °C

Electrical conductivity data of oxides at high temperatures (T > 1000°C) are rather scarce and generally inaccurate. For example, for α-alumina, the magnitude of conductivity determined by different authors varies by up to 4 orders of magnitude (Will, 1992). The difference between the results may be due to impurities and/or to different experimental

Always consult and cite the final, published document. See http://www.minsocam.org or GeoscienceWorld

conditions and procedures. The crucial point when measuring the conductivity is the choice of the electrode metal and configuration. At low temperature ($T < 800°C$), electrodes obtained by sputtering or painting the surface of the sample using Pt, Au or Ag metals generally give good and accurate results. Unfortunately, this method is not applicable at higher temperatures because of the disconnection of metal from the surface sample especially for single crystals where the surface is generally polished. Öijerholm et al (2006) studied the influence of different electrode configurations on the electrical conductivity of α-alumina ceramics and single crystals versus temperature. They concluded that above 700 °C, the spring-loaded Pt foil electrodes give accurate results and can be used for their simplicity. However, below 700 °C the surface conduction can have a significant influence on the measured conductivity for highly resistive oxides and the use of the so-called guarded electrodes (Macdonald, 1987) may be necessary to prevent such influence.

We used spring-loaded and unguarded electrodes in the temperature range 550 °C to 1400 °C. The sample was heated from room temperature up to 1400 °C using a rapid heating rate (400 °C/h), and then the temperature was held two hours at 1400 °C in order to obtain the maximum surface contact by sticking of the electrodes on the sample surface. The data acquisition did not show any increase of the electrical conductivity σ during the plateau at 1400 °C indicating the good contact electrodes/sample even before reaching 1400 °C. After slow cooling (120 °C/h) data were recorded by sweeping the frequency from 1 Hz to 1 MHz each 5 minutes. A second heating/cooling cycle was performed on each sample and showed a very good reproducibility of the conductivity results. Only data measured during decreasing the temperature are presented and discussed in this paper. In order to check the contact quality at low temperatures ($T < 700°C$), we used the standard method by sputtering Pt on both faces of the sample after the second cycle at high temperature. The comparison of the results between the two methods (Pt foils and sputtering Pt) show no significant difference

Always consult and cite the final, published document. See http://www.minsocam.org or GeoscienceWorld

suggesting that, on cooling the sample, stable electrode-sample contact is reached after the previous annealing at 1400 °C.

RESULTS

Frequency dependence of the electrical conductivity

In order to study the frequency dependence of the electrical conductivity of the single crystals, we used the Cole-Cole (or Nyquist) representation where we plot the opposite of the imaginary part of the complex impedance ($-Z''$) versus its real part (Z'). Two common behaviors against temperature were observed (Figure 2):

(1) At high temperatures (T > 900 °C), the plot consists of a semicircular arc at high frequencies (left part) and a spike at low frequencies (right part) the length of which increases with temperature. The left side arc is due to the dielectric relaxation process, while the spike is due to the well-known electrode polarization effects and is characteristic of ionic conductors (Grandjean 2006, Macdonald, 1987). The intersection of the curve with the real axis (Z''=0) gives the DC-resistance R_{DC} which is related to the static conductivity σ_{DC} by the relationship (Macdonald, 1987):

$$\sigma_{DC} = \frac{e}{S} \cdot \frac{1}{R_{DC}} \qquad (1)$$

where e is the thickness of the sample and S is the electrode surface area.

(2) At low temperatures (T < 900 °C), the left side arc still exists but the spike is replaced by a flat curve corresponding to Z''=0. For these low temperatures and high insulator materials, this flat curve cannot represent the electrode polarization effects. This purely resistive behavior should be a signature of an electronic conductivity. Such behavior has been observed for example in RuO_2-glass composites by Simonnet et al. (2004) who proved the mixed ionic and electronic character of the conductivity in their samples using DC-electrical measurements in the time domain. Unfortunately, this technique was not applicable in the case

Always consult and cite the final, published document. See http://www.minsocam.org or GeoscienceWorld

of our highly resistive samples where the signal versus time was in the order of the magnitude of noise due to the very low value of the DC-current generated in the sample. As we will see in the next section, the value of the activation energy for $T < 900$ °C is also in favor of mixed ionic and electronic conductors.

The circular arc (left side) can be fitted using an RC parallel circuit (Macdonald, 1987) which gives $R = 3 \cdot 10^6$ Ω, $C = 7 \cdot 10^{-12}$ F for $T = 800$ °C and $R = 1.6 \cdot 10^4$ Ω, $C = 2.2 \cdot 10^{-9}$ F for $T = 1300$ °C (Figure 2a and 2b). Using the same fit on the data reported by Chiekh et al (2001) on a single crystal (ZrO_2+9.5% mol Y_2O_3) at 300 °C we found $R = 1.7 \cdot 10^5$ Ω and $C = 5.2 \cdot 10^{-11}$ F. The comparison of the resistive part of the two samples shows that the mullite crystal is a better insulator than the yttria doped zirconia one.

Temperature dependence of electrical conductivity

Analyzing the frequency dependence of the electrical conductivity allowed us to determine the total DC-electrical conductivity $\sigma(T) = \sigma_{DC}(T)$ as a function of temperature. At high temperatures ($T > 900$°C), the conductivity $\sigma(T)$ is predominantly ionic and at low temperatures ($T < 900$°C), there is most probably an electronic contribution to the DC-conductivity. However, due to the highly resistive character of our samples, we were not able to separate each contribution (ionic and electronic) and its evolution with temperature.

Figure 3 shows the evolution of the DC-conductivity versus $10^4/T$ for the different orientations of the mullite single crystal sample. Applying the propagation of error formula (Ku, 1966) to equation 1:

$$\frac{\Delta\sigma}{\sigma} = \frac{\Delta e}{e} + \frac{\Delta S}{S} + \frac{\Delta R}{R} \qquad (2)$$

we estimate the error of the conductivity σ to ±5 % at the highest temperature ($T = 1400$ °C). At lower temperatures, however, the uncertainty of R increases because of the use of

Always consult and cite the final, published document. See http://www.minsocam.org or GeoscienceWorld

unguarded electrodes (Öijerholm et al., 2006). The estimated error bars of the conductivity σ are shown in Figure 3 only on the [001] orientation for some selected temperatures for clarity. The first important observation is that in the investigated temperature interval from 550 °C to 1400 °C the conductivity lies between about 10^{-9} Ω^{-1} cm^{-1} and 10^{-5} Ω^{-1} cm^{-1}. This means that mullite single crystal is an electrical insulator material even at high temperature ($\sigma \approx 1.3 \cdot 10^{-5}$ Ω^{-1}cm^{-1} at 1400°C). We also notice that the conductivity curve exhibits the same global trend for the three crystallographic directions with a change in the slope between $T \approx 850$ °C and $T \approx 950$ °C depending on the crystal orientation. In the low temperature range (LTR) the slope is lower than in the high temperature range (HTR).

In order to describe the evolution of the electrical conductivity with temperature T and to compare our results with previous ones, we used the "original" Arrhenius equation,

$$\sigma(T) = \sigma_0 \exp\left(-\frac{E_a}{kT}\right) \qquad (3)$$

where k is the Boltzmann constant, E_a is the activation energy associated with the transport mechanism and σ_0 is a pre-exponential factor. The obtained values of E_a and σ_0 for the three crystallographic orientations are summarized in Table 1. The rather low value of the activation energy (≈ 0.64 eV) observed in the LTR supports the assumption of a mixed ionic and electronic conductivity we already suggested by analyzing the frequency dependence of electrical conductivity, whereas the high value in the HTR is consistent with an ionic conductivity driven by oxygen ions associated to vacancies (see discussion).

DISCUSSION

Our experimental results clearly indicate that the electrical conductivity of mullite single crystal is controlled by two processes with different activation energies (Table 1). Below about 800 °C the conductivity is dominated by electronic contributions with the highest conductivity along [010] and with $\sigma_{[010]} > \sigma_{[100]} > \sigma_{[001]}$ ($\sigma_{av} \approx 5.4 \cdot 10^{-9}$ Ω^{-1}cm^{-1}, average

Always consult and cite the final, published document. See http://www.minsocam.org or GeoscienceWorld

conductivity at 550 °C). Above about 800 °C ionic conductivity becomes more and more important, particularly along the [001] direction, which eventually leads to an anisotropic electrical conductivity characterized by $\sigma([001]) > \sigma([100]) \approx \sigma([010])$. For example, at about 1400 °C the observed values are $\sigma_{[001]} = 1.31(7) \cdot 10^{-5}\Omega^{-1}\text{cm}^{-1}$, $\sigma_{[100]} = 1.01(5) \cdot 10^{-5}\ \Omega^{-1}\text{cm}^{-1}$ and $\sigma_{[010]} = 0.98(5) \cdot 10^{-5}\Omega^{-1}\text{cm}^{-1}$ ($\sigma_{av} \approx 1.1 \cdot 10^{-5}\ \Omega^{-1}\text{cm}^{-1}$, average conductivity at 1400 °C). The changing anisotropy of the electrical conductivity of mullite in the low and high temperature region can be clearly seen in Figure 4 where typical representation surfaces of the longitudinal electrical conductivity are shown. From the phenomenological point of view electrical conductivity can be considered a second rank tensor $\{\sigma_{ij}\}$ in first approximation. Following this, the longitudinal conductivity $\sigma(\mathbf{u})$ along an arbitrary direction $\mathbf{u} = u_i\mathbf{e}_i$, ($|\mathbf{u}| = 1$, $\mathbf{e}_i$ are the axes of the Cartesian reference system, i.e. $\mathbf{e}_1$//**a**, $\mathbf{e}_2$//**b** and $\mathbf{e}_3$//**c** in the case of orthorhombic mullite) is given by $\sigma(\mathbf{u}) = u_iu_j\sigma_{ij}$ (Einsteins sum convention applies).

Apart from the relatively low onset temperature of about 800 °C, the development of ionic conductivity with temperature fits well to the picture of a glass-like transition derived from anomalies observed in the temperature evolutions of heat capacity (Hildmann and Schneider, 2004), thermal expansion (Schreuer et al., 2006, Schneider et al., 2008), and elastic constants (Schreuer et al. 2006) for example. According to Schneider et al. (2008) the distribution of defects, namely the oxygen vacancies required for charge compensation and the triclusters (cf. Figure 1), is in a frozen-in state at low temperatures. At high temperatures hopping of oxygen atoms, bridging tetrahedral double chains (O(C) oxygen atoms) towards neighboring oxygen vacancies are possible. Gradual activation of this site-exchange processes leads to a glass-like static ↔ dynamic transition. According to this model, the onset of oxygen ion mobility and the correlated oxygen ion conductivity is associated with the observed discontinuous changes of the slopes of $\sigma(10^4/T)$. Because hopping of oxygen atoms can occur more easily between O(C) atoms and neighboring O(C) vacancies parallel to the **c**-axis than perpendicular to it, the anomaly in the σ versus $10^4/T$ curve occurs at lower temperatures (850

Always consult and cite the final, published document. See http://www.minsocam.org or GeoscienceWorld

± 20 °C) along [001] and at higher temperatures for directions within the (001) plane (890 ± 20 °C along [100] and 950 ± 20 °C along [010]). However, the small anisotropy of conductivities parallel and perpendicular to the crystallographic **c**-axis shows that oxygen hoppings have only a limited influence. This agrees well with the observation that oxygen diffusion in mullite displays no significant anisotropy (Fielitz et al. 2001a,b). The broad variation of the glass tranformation temperature ranging between about 850 °C derived from electrical conductivity and up to about 1200 °C from calorimetric experiments cannot be explained so far. It is not clear whether the different frequency regimes, and time and lengths scales of the experiments can account for the large spread.

The little impact of oxygen hoppings along to the crystallographic **c**-axis on the electrical conductivity can be explained by the complexity of site-exchange processes. The entering of an oxygen into a neighboring vacancy eliminates this vacancy by forming a new tetrahedral T-O(C)-T ($T = Al^{3+}$, Si^{4+}) bridge. This goes along with a migration of the TS* tricluster cations adjacent to the former O(C) oxygen vacancy to newly formed TS sites[2]. Simultaneously a new vacancy at the originally occupied O(C) site is produced (see Schneider et al. 2008, Figure 24). The latter requires a migration of the two tetrahedral TS atoms adjacent to the originally occupied O(C) atoms to the newly formed tetrahedral TS* tricluster sites. These structural rearrangements are much more sluggish than are simple O(C) hoppings and thus control the velocity of the whole process. The complex structural processes associated with these hoppings explain (i) the relative high values of activation energy in the high temperature conductivity region of mullite (≈ 1.6 eV) compared to that of Y_2O_3-doped ZrO_2 single crystal (≈ 0.82 eV) as reported by Filal et al. (1995) (note that in the paper of Filal et al., 1995, the value of activation energy is given as 0.90 eV because the authors considered a modified Arrhenius-type equation), and (ii) why the oxygen ionic conductivity in mullite is much lower than that of effective oxygen ion conductors like CaO- or Y_2O_3-doped ZrO_2 ($\sigma \approx 10^{-6}$ $\Omega^{-1}cm^{-1}$ for mullite instead of $\sigma \approx 10^{-1}$ $\Omega^{-1}cm^{-1}$ for 3%Y_2O_3-doped ZrO_2, both values for

Always consult and cite the final, published document. See http://www.minsocam.org or GeoscienceWorld

1100°C, see Figure 5). Furthermore, the complex structural processes of oxygen mobility make the high oxygen ionic conductivities beyond 1400°C as published by Rommerskirchen et al. (1994) rather unlikely. On the other hand due to the contribution of ionic conductivity the overall conductivity of mullite is higher than it is in high temperature insulators like α-alumina (at 1100 °C σ(mullite) $\approx 10^{-6}$ $\Omega^{-1}cm^{-1}$ instead of σ(α-alumina) $\approx 10^{-10}$ $\Omega^{-1}cm^{-1}$, Figure 5).

The mean electrical conductivity of mullite single crystals in the low temperature region displays a similar temperature-dependent behavior with comparable activation energies as that obtained by Chaudhury et al. (1999) from polycrystalline mullite ceramics, although the latter is significantly higher (Figure 6). The difference between both data sets is explained by the contribution of grain boundary effects to the overall conductivity in the case of ceramics caused by an enrichment of defects and impurities at the grain boundaries. In the high temperature region the difference between single crystal and polycrystalline ceramic data is continuously reduced with temperature and becomes almost zero at about 1400 °C (Figure 6). One reason of it may be the number of oxygen vacancies which are required for oxygen ionic conductivity. This number is higher in Al-rich 2/1-mullite single crystals (x = 0.4, corresponding to 2 oxygen vacancies per 5 unit cells) than in 3/2-mullite polycrystalline ceramics (x = 0.25, corresponding to 1 oxygen vacancy per 4 unit cells). The influence of grain boundaries probably is less important, since the free paths of ions and electrons between collisions is less than about 150 Å (see Kingery et al. 1975).

Always consult and cite the final, published document. See http://www.minsocam.org or GeoscienceWorld

REFERENCES CITED

Aryal, S., Rulis, P., and Ching,W.Y. (2012) Mechanical and electronic structure of mullite phases using first-principles modeling, Journal of the American Ceramic Society. 1-14.

Buchanan, R.C. (2004) Ceramic materials for electronics. Marcel Dekker.

Burnham, CW. (1964) Composition limits of mullite and sillimanite-mullite solid solution. Carnegie Institution of Washington Yearbook., 63, 223-227.

Chaudhuri, S.P., Patra, S.K., and Chakraborty, A.K. (1999) Electrical resistivity of transition metal ion doped mullite. Journal of the European Ceramic Society, 19, 2941-2950.

Cheikh, A., Madani, A., Touati, A., Boussetta, H., and Monty, C. (2001). Ionic conductivity of zirconia based ceramics from single crystals to nanostructured polycrystals. Journal of the European Ceramic Society, 21, 1837-1841.

Fielitz, P., Borchardt, G., Schmücker, M., Schneider, H., Widenbeck, M., Rhede, D., Weber, S. and Scherrer, S. (2001a) Secondary ion mass spectroscopy study of oxygen-18 tracer diffusion. Journal of the American Ceramic Society, 84, 2845-2848.

Fielitz, P., Borchardt, G., Schneider, H., Schmücker, M., Wiedenbeck M., and Rhede, D. (2001b) Self diffusion of oxygen in mullite. Journal of the European Ceramic Society, 21, 2577-2582.

Filal, M., Petot, C., Mokchah, M., Chateau, C., and Carpentier, J.L. (1995) Ionic conductivity of yttrium-doped zirconia and the "composite effect" Solid State Ionics, 80, 27-35.

Fischer, R.X and Schneider, H. (2005) The mullite-type family of crystal structures. In H.Schneider and S. Komarneni, Ed., Mullite, p. 1-46. Wiley-VCH, Weinheim.

Grandjean, A., Malki, M., and Simonnet, C. (2006) Effect of composition on ionic transport in SiO_2–B_2O_3–Na_2O glasses. Journal of Non-Crystalline Solids, 352, 2731–2736.

Guse, W. and Mateika, D. (1974) Growth of mullite single crystals ($2Al_2O_3 \cdot SiO_2$) by the Czochralski method. Journal of Crystal Growth, 22, 237-240.

Hildmann, B. and Schneider, H. (2004) Heat capacity of mullite. New data and evidence for a high-temperature phase transformation. Journal of the American Ceramic Society, 87, 227-234.

Jonscher, A.K. (1997) The 'universal' dielectric response. Nature, 267, 673-679.

Kingery, W.D., Bowen, H.K. and Uhlmann,D.R. (1975). Introduction to Ceramics. John Wiley and Sons, New York, pp 906-907.

Ku, H.H. (1966) Notes on the Use of Propagation of Error Formulas. Journal of Research of National Bureau of Standards, 70, 263-273.

Always consult and cite the final, published document. See http://www.minsocam.org or GeoscienceWorld

Macdonald, J.R. (1987) Impedance Spectroscopy: Emphasizing Solid Materials and Systems. Wiley, New York.

Mata-Osoro, G., Moya, J.S., Morales, M. Diaz, L.A., Schneider, H., and Pecharroman, C. (2012) Faradaic current in different mullite materials: single crystal, ceramic and cermets. International Journal of Materials Research, 103, 408-411.

Öijerholm, J., Pan, J., and Leygraf, C. (2006) In-situ measurements by impedance spectroscopy of highly resistive α-alumina, Corrosion Science, 48, 243-257.

Rommerskirchen, I., Chavez, F., and Janke, D. (1994) Ionic conduction behavour of mullite ($3Al_2O_3 \cdot 2SiO_2$) at 1400 to 1600°C. Solid State Ionics, 74, 179-187.

Rüscher, C.H., Shimada, S., and Schneider, H. (2002) High-temperature hydroxylation of mullite. Journal of the American Ceramic Society, 85, 1616-1618.

Schneider, H. and Komarneni, S. (2005) Mullite, p.1-487, Wiley-VCH, Weinheim.

Schneider, H., Schreuer, J., and Hildmann, B. (2008) Structure and properties of mullite – a review. Journal of the European Ceramic Society, 28, 329-344.

Schreuer, J., Hildmann. B., and Schneider, H. (2006) Elastic properties of mullite single crystals up to 1400°C. Journal of the American Ceramic Society, 89, 1624-1631.

Simonnet, C., Grandjean, A., Malki, M. (2004) Mixed ionic and electronic conductivity of oxides from molten state to glassy state: application to RuO_2-glass composites. Solid State Ionics, 175, 695–698.

Will, F.G., de Lorenzi, H.S., and Janora, K.H. (1992) Conduction mechanism of single-crystal alumina, Journal of the American Ceramic Society, 75, 295-304.

Always consult and cite the final, published document. See http://www.minsocam.org or GeoscienceWorld

FIGURE CAPTIONS

Figure 1. Crystal structure of mullite in comparison to that of sillimanite in projections parallel [001] (above) and parallel [100] (below). The structure plots of mullite give a schematic and simplified view of the oxygen vacancies and the tetrahedral triclusters (see the text).

Figure 2. Cole-Cole (or Nyquist) plots for the crystal [001] at two temperatures (a) T = 800 °C and (b) T = 1300 °C. Z' and Z'' represent the real and the imaginary parts of the complex impedance, respectively. Scatters represent the experimental points and solid lines the fit of the circular arc (left side) using an RC parallel circuit (see text).

Figure 3. Arrhenius plot of the DC conductivity for the three mullite single crystals. Solid lines represent the fit of the experimental points using equation 2 (see text).

Figure 4. Representation surfaces of longitudinal electrical conductivity of mullite single crystal at 550 °C (left) and 1400 °C (right). Units of axes are $10^{-9}\Omega^{-1}cm^{-1}$ and $10^{-6}\Omega^{-1}cm^{-1}$, respectively.

Figure 5. Comparison of the electrical conductivity of the single crystals: mullite [001] (this work), pure alumina [001] (Will et al., 1992) and 3% Y_2O_3-doped ZrO_2 (Filal et al., 1995).

Figure 6. Comparison between the mean electrical conductivity of the three orientations of our mullite single crystals and the conductivity of the mullite ceramic reported by Chaudhury et al. (1999).

Always consult and cite the final, published document. See http://www.minsocam.org or GeoscienceWorld

This is a preprint, the final version is subject to change, of the American Mineralogist (MSA)
Cite as Authors (Year) Title. American Mineralogist, in press.
(DOI will not work until issue is live.) DOI: http://dx.doi.org/10.2138/am.2014.4442

Table 1

	[001] LTR	[001] HTR	[100] LTR	[100] HTR	[010] LTR	[010] HTR
E_a (eV)	0.68 ± 0.12	1.64 ± 0.04	0.64 ± 0.12	1.64 ± 0.04	0.64 ± 0.17	1.57 ± 0.06
log(σ_0)	-4.36 ± 0.26	0.01 ± 0.05	-4.45 ± 0.26	-0.13 ± 0.05	-4.25 ± 0.26	-0.33 ± 0.05

Table 1. Activation energy (Ea) and pre-exponential factor (log(□0)) values for the electrical conductivity along to [001], [100] and [010] of mullite in low temperature region (LTR) and in high temperature one (HTR).

This is a preprint, the final version is subject to change, of the American Mineralogist (MSA)
Cite as Authors (Year) Title. American Mineralogist, in press.
(DOI will not work until issue is live.) DOI: http://dx.doi.org/10.2138/am.2014.4442

Figure 1

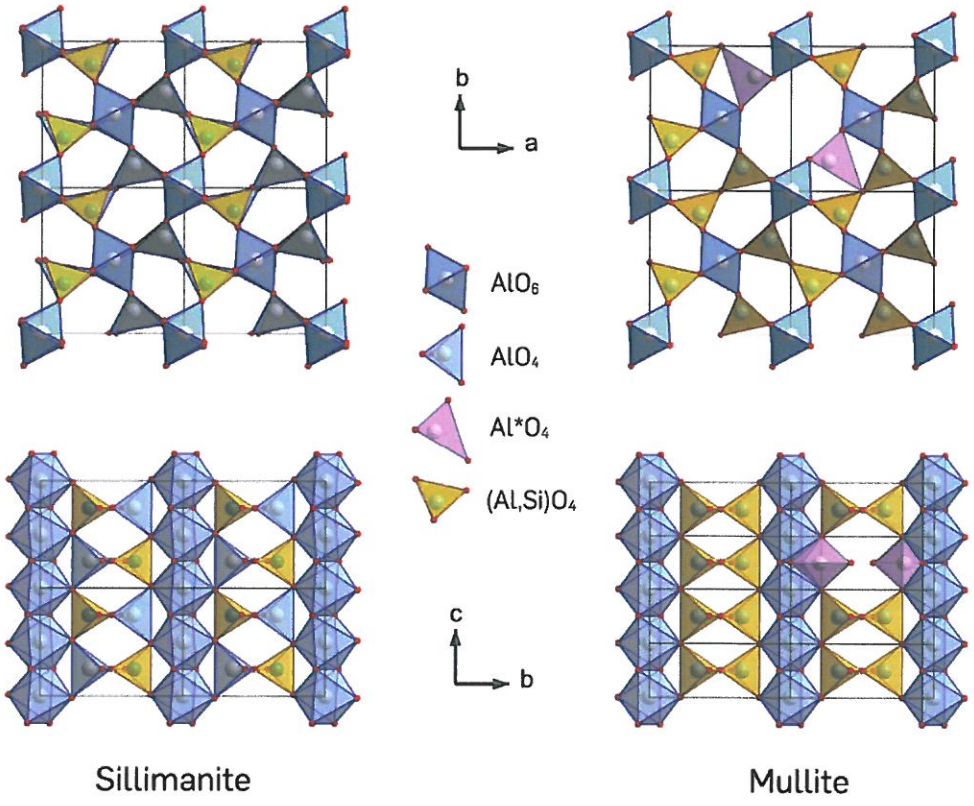

Figure 1. Crystal structure of mullite in comparison to that of sillimanite in projections parallel [001] (above) and parallel [100] (below). The structure plots of mullite give a schematic and simplified view of the oxygen vacancies and the tetrahedral triclusters (see the text).

Always consult and cite the final, published document. See http://www.minsocam.org or GeoscienceWorld

Figure 2

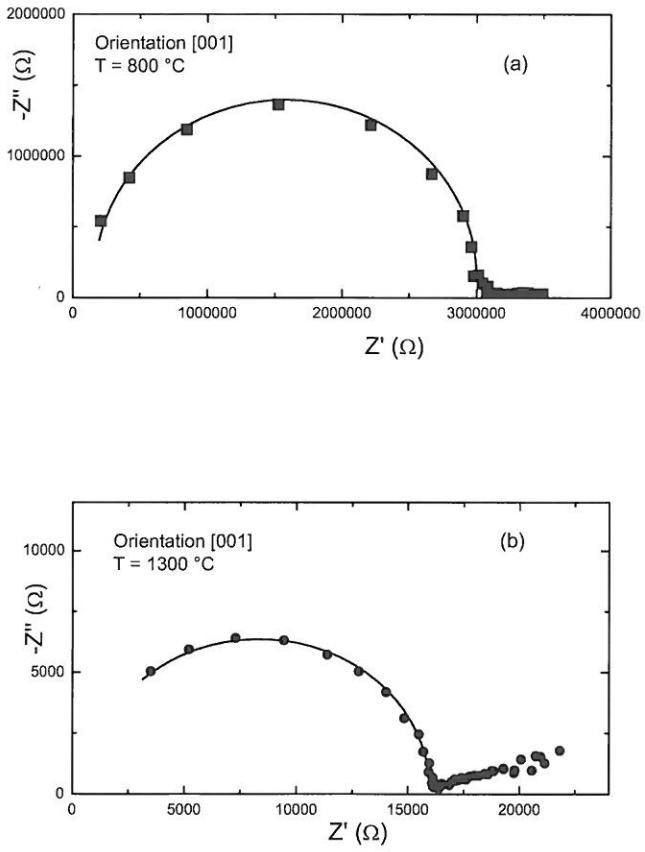

Figure 2. Cole-Cole (or Nyquist) plots for the crystal [001] at two temperatures (a) T=800 °C and (b) T = 1300°C. Z' and Z" represent the real and the imaginary parts of the complex impedance respectively. Scatters represent the experimental points and solid lines the fit of the circular arc (left side) using an RC parallel circuit (see text).

This is a preprint, the final version is subject to change, of the American Mineralogist (MSA)
Cite as Authors (Year) Title. American Mineralogist, in press.
(DOI will not work until issue is live.) DOI: http://dx.doi.org/10.2138/am.2014.4442

Figure 3

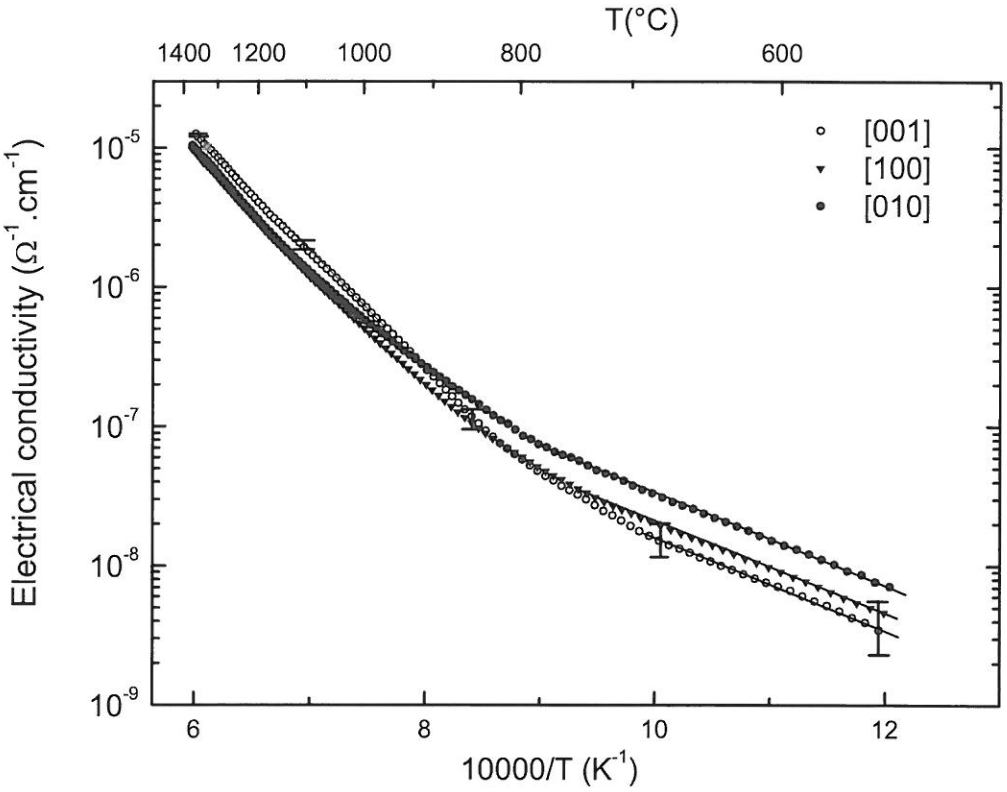

Figure 3. Arrhenius plot of the dc conductivity for the three mullite single crystals. Solid lines represent the fit of the experimental points using equation 3 (see text).

Always consult and cite the final, published document. See http://www.minsocam.org or GeoscienceWorld

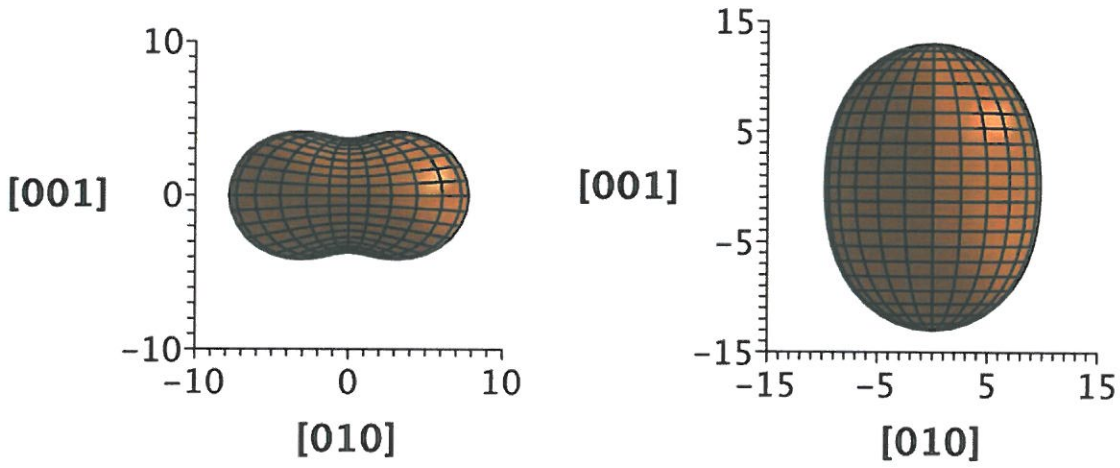

Figure 4. Representation surfaces of longitudinal electrical conductivity of mullite single crystal at 550 °C (left) and 1400 °C (right). Units of axes are $10^{-9}\Omega^{-1}cm^{-1}$ and $10^{-6}\Omega^{-1}cm^{-1}$, respectively.

Figure 5

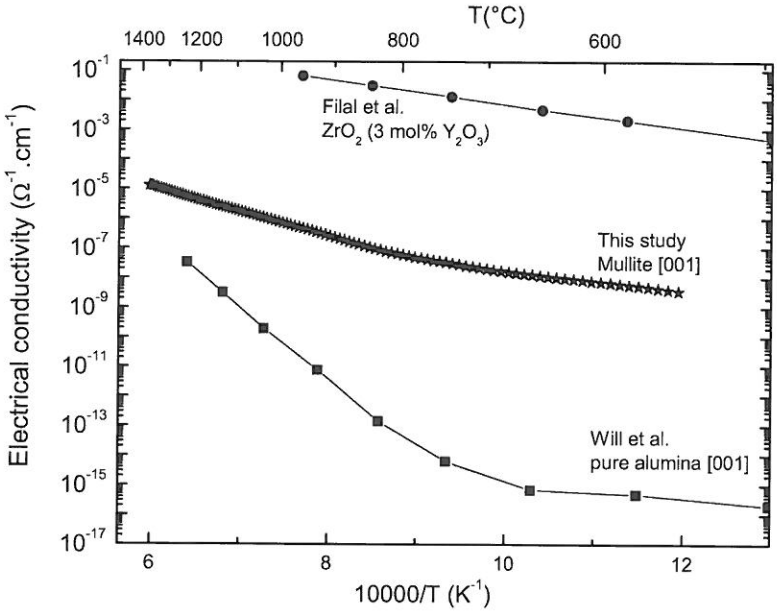

Figure 5. Comparison of the electrical conductivity of the single crystals: mullite [001] (this work), pure alumina [001] (Will et al. 1992) and 3%$Y2O_3$-doped ZrO_2 (Filal et al. 1995).

This is a preprint, the final version is subject to change, of the American Mineralogist (MSA)
Cite as Authors (Year) Title. American Mineralogist, in press.
(DOI will not work until issue is live.) DOI: http://dx.doi.org/10.2138/am.2014.4442

Figure 6

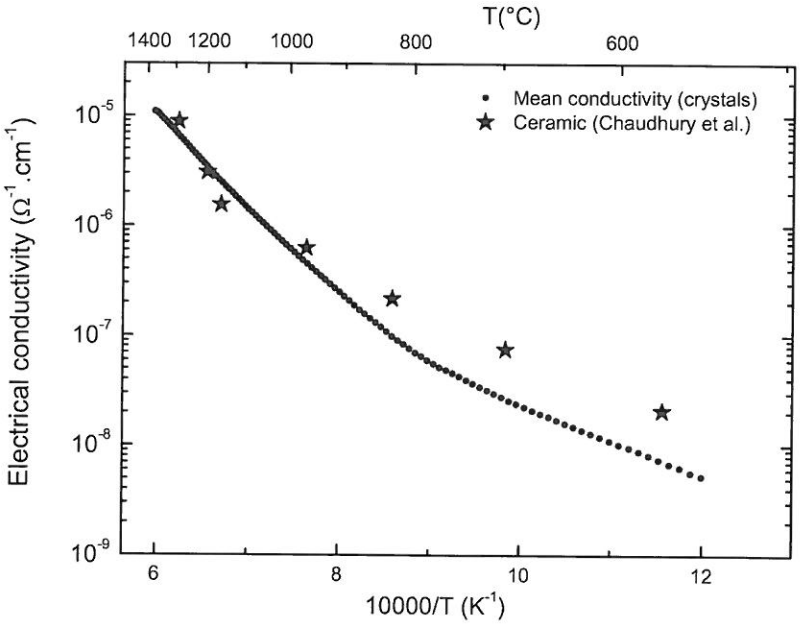

Figure 6. Comparison between the mean electrical conductivity of the three orientations of our mullite single crystals and the conductivity of the mullite ceramic reported by Chaudhury et al (1999).

Always consult and cite the final, published document. See http://www.minsocam.org or GeoscienceWorld